IIETA International Information and Engineering Technology Association
Advancing the World of Information and Engineering

Revue des Composites et des Matériaux Avancés-Journal of Composite and Advanced Materials
Vol. 34, No. 5, October, 2024, pp. 653-660
Journal homepage: http://iieta.org/journals/rcma

Study of Behaviour and Morphology of Corrosion Region of Copper Layer Coated on Polymer Substrates by Flame Thermal Spraying

Ghufran J. Matrood*, Niveen J. Abdulkader, Nahedh M. Ali

Department of Materials Engineering, University of Technology - Iraq, Baghdad 10069, Iraq

Corresponding Author Email: mae.19.41@grad.uotechnology.edu.iq

Copyright: ©2024 The authors. This article is published by IIETA and is licensed under the CC BY 4.0 license (http://creativecommons.org/licenses/by/4.0/).

https://doi.org/10.18280/rcma.340513

Received: 19 September 2024
Revised: 14 October 2024
Accepted: 23 October 2024
Available online: 31 October 2024

Keywords:
metallization, pure Cu, HDPE, ABS, pull-off test, corrosion resistance

ABSTRACT

Metallization of polymers is a modern technique used to improve their properties by coating them with conductive, lightweight surfaces, enabling their use in many electronic and communications applications. This study examines the effect of corrosion of a copper layer deposited on two polymeric substrates, high-density polyethylene (HDPE) and acrylonitrile butadiene styrene (ABS), by flame thermal spraying. Pull off test shows the adhesion strengths between the Cu coating layers and the HDPE and ABS substrates were 1.42 and 1.94 MPa, respectively. The contact angles for the HDPE and ABS were 57.227 and 36.422°, respectively, indicating that the ABS substrate is more wettable than the HDPE substrate. A corrosion test of the coated substrates was conducted at 27±1 °C in a solution of 3.5% NaCl. The corrosion rate was 2.763×10^{-2} mm/year for Cu on HDPE and 1.361×10^{-2} mm/year for Cu on ABS. The corrosion rate of Cu on HDPE is greater than that of Cu on ABS, indicating that the Cu coating layer on the ABS substrate is denser and less porous than that on the HDPE substrate. The corrosion products for the corroded Cu layer on HDPE were NaCl, NaOH, Cu_5Zn_8 and CuCl, whereas those for the corroded Cu on ABS were CuCl and $Cu(OH)_2$.

1. INTRODUCTION

Polymer metallization is an emerging area of study that aims to combine the advantageous features of metal coatings with those of plastic substrates [1]. The materials used for a wide range of contemporary manufactured products are selected based on the characteristics that make them suitable for the intended purpose of the products. Polymers exhibit corrosion resistance and resistance to a wide range of common chemicals and are also lightweight. However, they lack the hardness of metals and have low thermal and electrical conductivity [2-4]. The numerous applications of metallized polymers range from microelectronics to food packaging [5, 6]. Copper, which has lower resistivity than aluminium, is expected to gradually replace aluminium in future devices owing to the need for further miniaturization and reduction of the propagation delay. Polymers are also considered possible low-permittivity (low-k) dielectrics, even for on-chip interconnects [7].

Thermal spraying is when a molten or partially molten material is applied to a surface using a high-velocity spray to create a coating. When the coating particles come into contact with the substrate surface, they undergo permanent deformation, forming a coating layer. The coating material can be employed in either a powder or wire form. Oxygen and acetylene (C_2H_2) are the gases used to generate heat in thermal spraying. The flame induces rapid melting of the coating material, which is then violently ejected onto the substrate surface [8-10].

The adhesive qualities of coating materials are essential because adhesion is a vital attribute [11]. The adhesive quality directly influences their functionality when used as coatings on substrates [12]. The adhesion of coatings depends on their chemical and physical characteristics [11, 12]. Essentially, layers containing polar functional groups can adhere to metal substrates, usually by secondary bonding and sometimes through primary bonding [12]. However, the fundamental chemical interactions between coating materials and substrates may be insufficient to produce good outcomes. As a result, various surface pretreatments, such as sandblasting and phosphating, are used to improve mechanical adhesion [13]. Moreover, wetting phenomena are affected by the energy of the substrate surface, which impacts adhesion [12, 13]. In addition, several practical considerations impact the adhesive qualities, including the thickness of the coating [13], the thermo-mechanical characteristics of the film, the application process and the substrate pretreatment measurement [12].

Corrosion, which is the deterioration of a metal due to a chemical or electrochemical reaction with its environment, is one of the main reasons for the failure of engineered components and structures [13, 14]. When a material, often a metal, reacts with its environment, a process known as corrosion occurs, causing the material and its properties to deteriorate. The environment affects the material's corrosion behaviour, and vice versa; the corrosive impact of an environment depends on the material [15]. Thus, it is essential to clarify a material's corrosion resistance before its design for

a particular application.

Corrosion processes significantly affect the reliability of electronic components [16-18]. Corrosion manifests in metallic materials when exposed to moisture and reactive gases, including sulfur dioxide and nitrogen oxides. Aggressive substances such as halides, including chlorides, significantly enhance corrosion processes. These processes result in the impairment of material properties due to chemical reactions. Electrochemical reactions are consistently involved in electro-conductive materials and frequently play a critical role. Electronic materials and components are particularly impacted due to exposure to increasingly harsh environmental conditions, leading to damage from corrosive media, such as in offshore systems and electronic components within automobile engine compartments. Corrosion-induced processes are significant reliability limitations for the materials and contacts of micro- and power electronic components [19].

Because of its outstanding electrical and thermal conductivity, copper has been extensively utilized in many different applications, including electronic devices and temperature exchange. Further, owing to its relatively high resistance to atmospheric corrosion, it has been widely used in the production of artworks and the construction of architectural components such as gutters and roofs [15, 20-24]. In addition, copper provides adequate protection against corrosion in near-neutral or alkaline environments due to the spontaneous formation of a passive layer on its surface [25, 26]. The International Organization for Standards recommends using copper as a sensor for detecting corrosion due to atmospheric chemicals [27].

Nanotechnology is considered to significantly influence nearly every aspect of human life. It possesses the capacity to profoundly impact many domains, including physical sciences, biotechnology, energy, communication technology, social psychology, manufacturing, catalysis, computational sciences, and transportation. It can revolutionize the future by increasing the durability and reactivity of existing materials [28-30].

Acrylonitrile butadiene styrene (ABS) is a thermoplastic material with several applications in engineering because of its advantageous properties, including its chemical resistance, lightweight, mechanical strength, and ease of processing [31]. High-density polyethylene (HDPE) is a semi-crystalline material and the most widely used plastic. It is rigid and more abrasion—and heat-resistant [32].

Devaraj et al. [33] investigated the adhesive qualities of copper, aluminium and zinc coatings deposited on porous polyethylene by wire arc spraying. They found that all three metallic coatings had bond strength exceeding the ultimate fracture strength of the porous polyethylene. These results indicate that holes in the polymer significantly reduce its weight and help to solve problems related to the metallization of polyethylene, resulting in the formation of a very lightweight composite material with potential uses in heat control.

Voyer et al. [34] employed cooling air to cool a polymer substrate used for deposition by flame spraying. They found that the use of cooling air and the adjustment of spraying settings can reduce the distance between the flame torch and the substrate without generating thermal damage to the polymer substrate, which can be easily confirmed visually. Thus, flame-sprayed coatings may influence the electrical characteristics of a polymer substrate even if the deposition technique does not affect the structural integrity of the sprayed constructions. Ashrafizadeh et al. [35] The Coating electrical resistance of the coating was being reduced by adding compressed air, which decreased the porosity of the Al-12Si layer owing to the increase. The use of compressed air enhances the impact velocity of the sprayed particles and their enhanced deformation. It is possible to demonstrate that a constant substrate temperature can be maintained by reducing the distance between the substrate and the spray gun and increasing the compressed air's ejection pressure and flow rate. To obtain thick layers of Al-12Si, it is necessary to reduce the distance between the substrate and the spray gun.

Huang et al. [36] applied a yttrium-stabilized zirconia (YSZ) coating to a fibre-reinforced polyimide substrate after using aluminium as a bond coat to protect the substrate from the extremely high temperatures of the plasma-sprayed YSZ deposition particles. Moreover, they demonstrated how the heat insulation for the polymer substrate was improved by using Zn as a bond coat. The lower thermal conductivity of Zn of 116 W/m-K than that of Al (approximately 237 W/m-K) likely explains the improved heat insulation. The application of the Zn bond coat enhanced the thermal shock resistance of the final deposited coating compared with that of the Al bond coat. Therefore, applying an appropriate bond coat to polymers helps to reduce the negative thermal effects of thermal spray metallization.

By reviewing the previous literature, it became clear that researchers studied the obstacles in the metallizing process that cause deformation of the polymers during the coating process, which will be treated in our research through the use of nano copper and nano Zn bond coat, as well as the use of compressed air to prevent excessive heat of polymers substrate, which causes deformation of the polymer and weakens the adhesion between the coating layer and the polymer substrate material.

The main motivations for using metallized polymers in the production of electronic devices are to reduce costs, decrease weight, and enhance electrical conductivity. In this study, two polymers were metallized with Cu to obtain lightweight products with electrical conductivity, and the corrosion resistance of the coating layer was studied.

2. EXPERIMENTAL PROCEDURE

2.1 Materials used

Table 1. Chemical composition of pure Cu

Element %	Chemical Composition
P	0.008
Pb	0.0001
Ag	0.0002
Sn	0.0006
Fe	0.003
Mn	0.0006
Bi	0.004
Si	0.001
Zn	0.008
Cu	99.9

ABS and HDPE with dimensions of 4 × 2 cm^2 were used as the substrates. Copper powder with 99.9% purity and a particle size of 130.9 nm was used as the coating material, and zinc powder with a particle size of 65.5 nm was used as the bond

coat. The chemical compositions of the Cu and Zn powders are presented in Tables 1 and 2.

Table 2. Chemical composition of Zn

Element %	Chemical Composition
Fe	0.0561
Ti	0.044
Cu	0.0631
Mg	0. 022
Mn	0.0391
Si	0.0044
Zn	99.8

2.2 Coating process

Before the coating process, the ABS and HDPE substrates were cleaned using NaOH, then sandpaper was used to roughen them. The coating was then performed using two torch flame spray devices. A torch flame was used to melt the zinc particles, which were atomized by compressed air. The semi-molten particles were then deposited on the polymeric substrate, thus forming a zinc bond coat. After that, Cu particles are semi-melted and then atomized over the zinc bond coat to create a Cu top coat. The reason for using a Zn bond coat is to prevent the direct impact of semi-molten Cu particles with polymer, which causes polymer degradation. Combustion gases and auxiliary compressed air were used to provide the necessary particle velocity. Air cooling was used to avoid the polymer's degradation and increase the adhesion force between the polymeric substrate and the metallic coating.

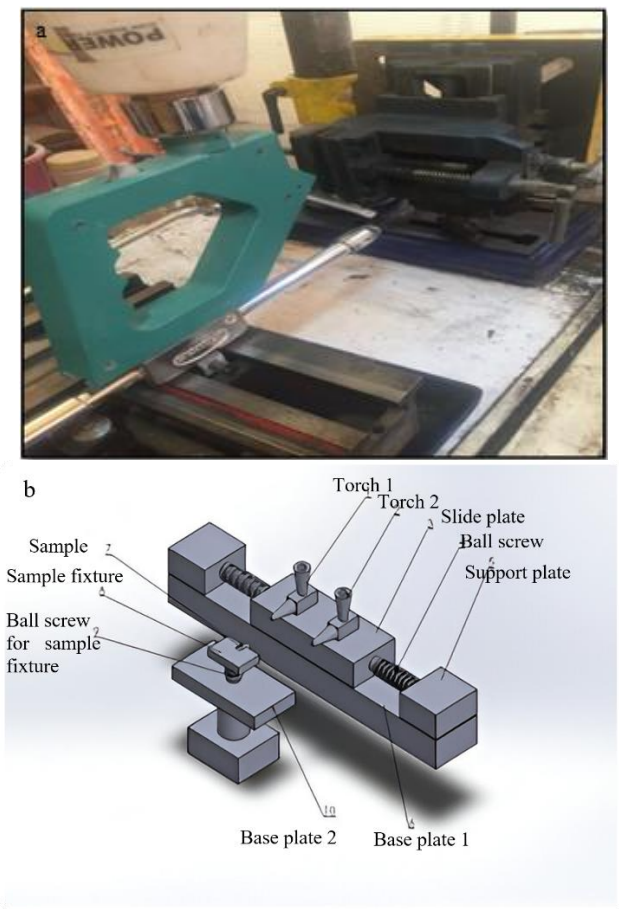

Figure 1. a) Two torch flame spray device, b) Diagram for thermal spraying device

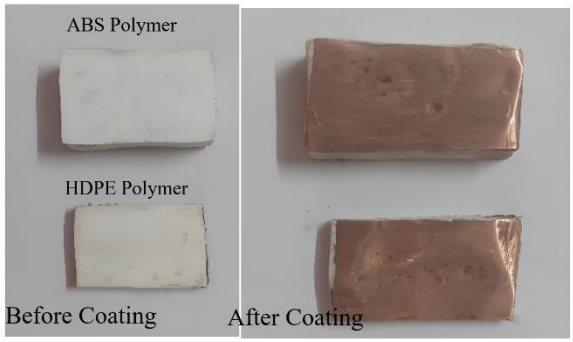

Figure 2. The samples before and after the coating process

The parameters of the metallization process were a distance of 250 mm between the polymeric substrate and the spray gun, 45 g of feeding powder, a spray velocity of 200 m/min and a delay time of 4 min [37]. The pressures of O_2 and C_2H_2 used to generate heat in the thermal spraying were 0.5 and 1 bar, respectively [38]. The two torch flame spray devices, diagram for thermal spraying device, and the samples before and after the coating process are illustrated in Figures 1 and 2, respectively.

2.3 Characterization and test

2.3.1 Contact angle test

One of the most common approaches to determining the wettability of a surface or substance is to calculate the contact angle. The process of wetting refers to how a liquid spreads across a solid surface or the ability of a liquid to generate an interface with a solid object. The wettability was measured at the Department of Chemical Engineering, University of Technology, Baghdad.

2.3.2 Pull-off test

The effectiveness of a coating and its bonding to a substrate can be evaluated using a pull-off test device. Pull-off tests of the coated substrates were performed at the ACT Company, Basra, Iraq. Before applying the adhesive in the tests, the samples were ground using sandpaper to roughen them. Then, as illustrated in Figure 3, dolly adhesive was applied to the coating layer and a load was applied until the coating adhesion failed.

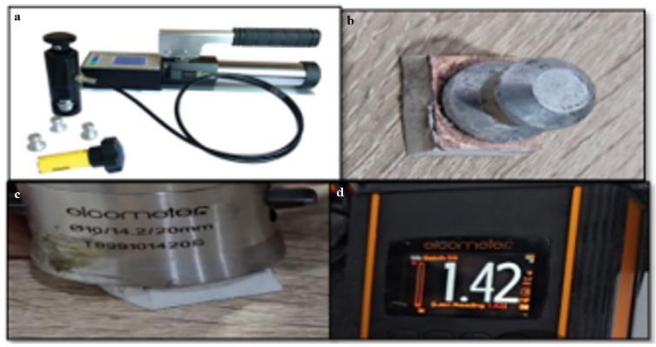

Figure 3. a) Pull-off test device, b) doll adhesive is placed with the coating layer, c) load is provided into the doll, d) the result of pull off test

2.3.3 Corrosion test

A standard immersion corrosion test (DY2300 POTENTIOSTAT) was used to investigate the corrosion rates

of the Cu coating layer. A corrosion test was performed to determine the rate of corrosion of the copper coating. Test specimens of each material were ground with sandpaper of various grits (800–2000), washed with distilled water and methanol, and dried. The caustic mixture used in the corrosion test was composed of distilled water and 3.5% sodium chloride. The test was performed at a temperature of 27±1°C. Anodic and cathodic polarization are typically used in a corrosion test to induce metal dissolution (corrosion) and passivation. This approach uses an externally provided variable electric current to complete the experiment quickly. The stationary corrosion condition of a Tafel equation is the intersection of the anodic and cathodic polarization curves. Figure 4 shows the diagram for the corrosion device.

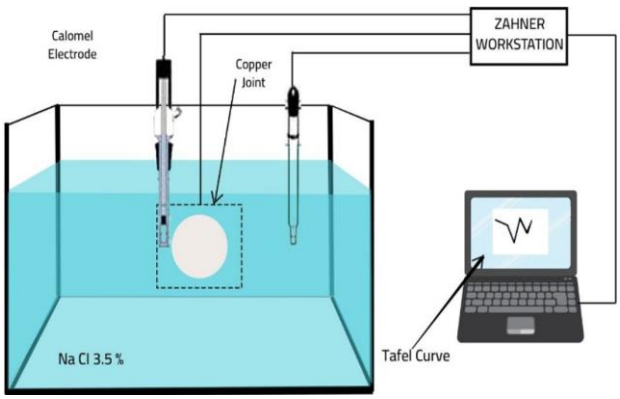

Figure 4. Corrosion device

2.3.4 X-RAY diffraction

The phase and crystallinity of copper coated structures were measured at room temperature with a X-ray Diffractometer working in $\theta = 2\theta$ scanning mode and using a K copper radiation source (λ = 1.5406 A). The obtained diffraction patterns were analyzed through the data evaluation program. The X-ray diffraction test was performed at the Nanotechnology and Advanced Materials Research Centre of the University of Technology, Baghdad, using Shimadzu XRD 6000 X-ray diffraction equipment.

2.3.5 Scanning electron microscopy

Scanning electron microscopy using a Thermo Scientific SEM equipment at AlKora Company allowed one to investigate the structure of the coating layer of every sample.

2.3.6 Electrical conductivity test

The electrical conductivity of the coating layers was measured using an LCR-821 meter. At the Department of Materials Engineering of Technical College, Baghdad.

3. RESULTS AND DISCUSSION

The angle between the liquid-solid and liquid–vapour interfaces is called the contact angle [39]. The contact angle of the HDPE samples was 57.227°, higher than that of the ABS samples (36.422°), as shown in Figure 5, indicating that the surface of the ABS substrate was more hydrophilic than that of the HDPE substrate and thus had more excellent wettability and adhesiveness. This result could be due to the smoothness of the HDPE surface, the non-polarity of the HDPE structure owing to the long CH_2 chains, the low surface energy resulting from the lack of polar groups, and the hydrophobic character inhibiting its interaction with polar water molecules [40].

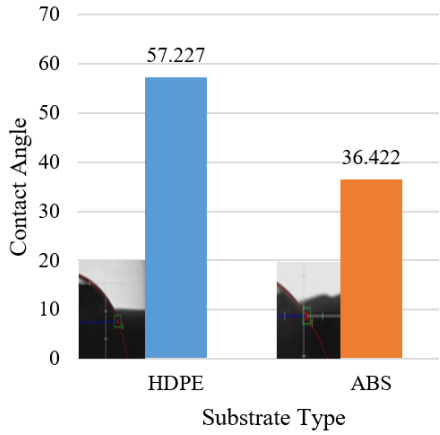

Figure 5. Contact angle of substrate materials

The pull-off test is a popular method of evaluating the adhesion strength [41-43]. The adhesion strengths between the Cu coating layer and the HDPE and ABS substrates were 1.42 and 1.94 MPa, respectively. The mechanical interlocking between the coating and substrate is achieved by *in situ* structuring of the substrate during the application of the coating. This requires precise control of the heat input into the substrate and the particle impact.

A few different types of sample failure may be identified in a pull-off test: adhesive failure at the interface surface; cohesive failure inside the coating, substrate or glue; and mixed failure. The test panel and the dolly still had a coating after failure, indicating that cohesive failure occurred in all the samples examined [44].

The electrical conductivity of the Cu on the HDPE and ABS substrates was 4.746×10^4 and 5.589×10^4 $\Omega^{-1}.cm^{-1}$, respectively. In comparison, the electrical conductivity of bulk copper was 5.96×10^5 $\Omega^{-1}.cm^{-1}$. The reason for the lower electrical conductivity of the Cu coating layer than that of the copper is that the nanoparticles in the coating layer increased the number of grain boundaries [45]. The difference between the electrical conductivities of the Cu coating layer on the HDPE and ABS polymeric substrates is due to the denser and less porous Cu coating layer on the ABS than that on the HDPE [46].

Table 3. Corrosion parameters of Cu layer

Substrate	HDPE	ABS
Coating layer	Cu	Cu
Ecorr (V)	-0.889	-0.347
βa (V)	0.478	0.097
βc (V)	-0.249	-0.572
I_{corr} $(\mu A/cm^2)$	10^{-5}	1.266×10^{-5}
Corrosion rate(mm/year)	2.763×10^{-2}	1.361×10^{-2}
i	2.349×10^{-6}	1.157×10^{-5}

The corrosion parameters are presented in Table 3. According to the Tafel diagram in Figure 6 for the copper coating on the HDPE and ABS polymeric substrates, the cathode current increases gradually and steadily, leading to a greater negative voltage. When electrons are abundant, the cathode current rises, stimulating reduction. The reduction current drops beyond a certain point owing to mass transfer constraints on the reactant surface at substantially negative potentials; the voltage is sufficient to allow the reaction, but

materials cannot quickly reach the electrode surface to sustain the current.

The corrosion behaviour of the coating layer is similar to that of the cathodic and anodic reactions. However, the corrosion rate on the HDPE substrate is higher than that on the ABS substrate, which indicates that the coating layer on the ABS substrate is denser and less porous than that on the HDPE substrate.

Since copper is only resistant to corrosion in the passive state depending on the solution pH and component [47], the passivation process is crucial. It can be considered that the weakly conducting passive layer covering the Cu-coated surface further inhibits the corrosion reaction. Due to copper dissolution, the potential–current density plots of the two coatings evaluated in this study indicated an increase in the anodic current density. There is a break in this growth due to the production of complicated corrosion products on the surface of the coating.

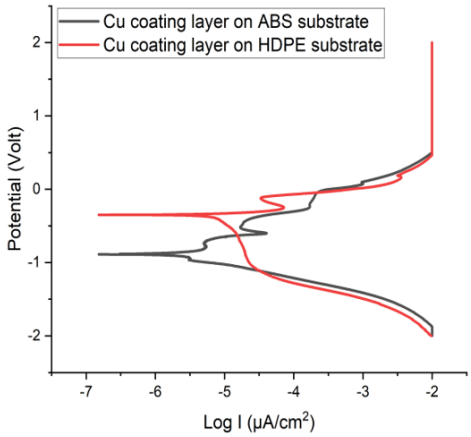

Figure 6. Tafel diagram of Cu layer on HDPE and ABS polymers

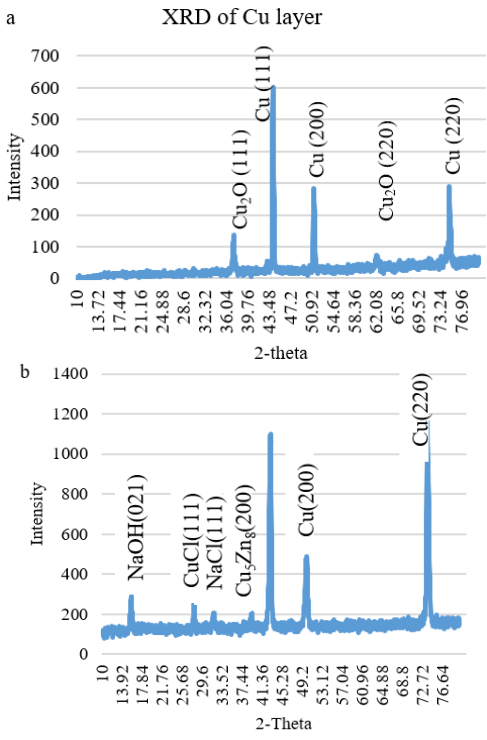

Figure 7. XRD of Cu layer on HDPE substrate, a) before corrosion, b) after corrosion

The XRD data in Figure 7(a) indicate diffraction peaks at 2-theta values of 44.1, 51.33 and 74.8°, corresponding to (111), (200) and (220) diffraction peaks of the Cu coating on the HDPE, respectively. In addition, the two diffraction peaks at 37.3 and 62.2° were indexed to (111) and (220) peaks of cuprous oxide (Cu_2O), respectively. The presence of Cu_2O suggests partial oxidation of the Cu layer. Figure 7(b) shows the XRD data of the Cu coating layer after the corrosion test. Corrosion products such as NaCl, NaOH, Cu_5Zn_8 and CuCl were observed on the corroded Cu layer deposited on the HDPE. The debye-Scherrer formula is used to calculate the average crystalline size. From the half-width of the (111) diffraction peak, the average size of the crystallites was calculated to be 454.9 nm before the corrosion test and 377.87 nm after the corrosion test.

Figure 8(a) shows the XRD data for the Cu layer on ABS, where the diffraction peaks correspond to (111), (200) and (220). Corrosion products such as CuCl and $Cu(OH)_2$ were observed in the corroded Cu layer deposited on ABS, as shown in Figure 8(b). The average crystalline size was calculated to be 454 nm before the corrosion test and 324.5 nm after the corrosion test from the half-width of the (111) diffraction peak.

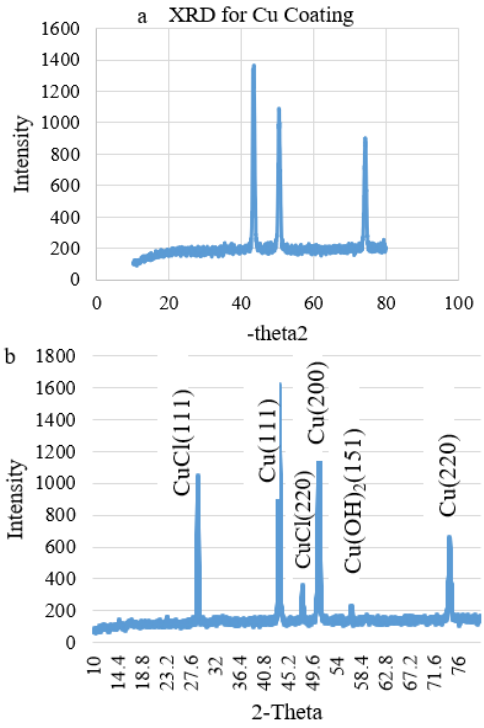

Figure 8. XRD of Cu layer on ABS substrate, a) before corrosion, b) after corrosion

Corrosion reduced the grain size because the grain became weaker as the depth of the pits and the pit density increased, in turn weakening the entire structure. This resulted in the granules being divided into smaller pieces [1].

Figure 9 shows the interface between the polymer substrate and the Cu coating layer before the corrosion test. The SEM image indicates that the coating layer on the sample surface has a smooth and homogeneous structure, increasing its corrosion resistance.

The percentage porosity of the Cu layers on the HDPE and ABS substrates was determined using ImageJ software to be 7% and 4%, respectively, indicating that the Cu layer on the ABS substrate was denser than that on the HDPE substrate.

Figure 9 shows the interface between the polymer substrate and the Cu layer.

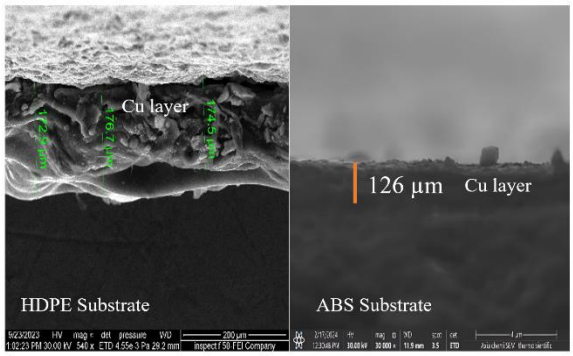

Figure 9. The interface between polymer substrate and Cu layer

SEM was used to examine the surface morphology of the Cu-coated substrates to evaluate the surface of each coating after corrosion to determine its effects. The surface was rough and the Cu layer had peeled off. The corrosion layer, as shown in Figures 10 and 11, was in the form of flaky of different sizes depending on the severity of the corrosion of the solution with the coating layer. This led to it collecting on the surface and not dissolving in the solution. The anodic reaction is the electron loss process—also known as the copper's dissolving process. The oxygen's depolarisation response forms the cathodic reaction. Thus, the corrosion primarily results in copper oxide. When the chloride ion in the salt dissolves into a thin film of liquid, it sticks to the metal's surface or the passivated film. This creates a strong electric field that damages the oxide coating on the surface and speeds up the metal's dissolution. The chloride ions can enter the matrix through the passivation layer, combine with the copper element to form soluble $CuCl_2$, and then react with oxygen to form Cu_2O, $CuCl_2$, and $_3Cu\ (OH)_2$ [48].

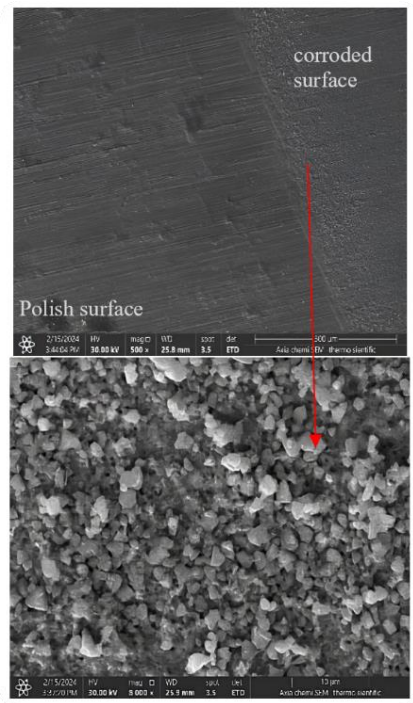

Figure 10. SEM for the Cu layer on HDPE after the corrosion test

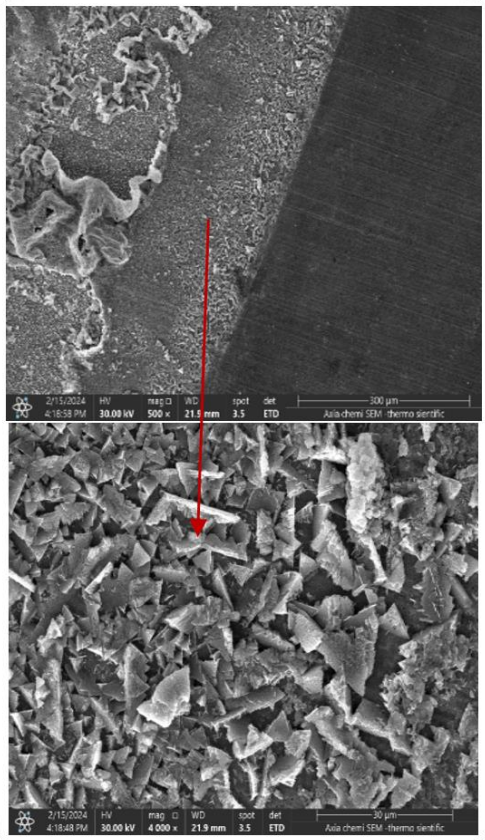

Figure 11. SEM for the Cu layer on ABS after corrosion test

Figure 10 shows the Cu coating layer on the HDPE substrate after the corrosion test. It can be observed that the surface broke down and became rough because of deposited of corrosion product in the form of flaky layer.

As illustrated in Figure 11, a high surface roughness resulted from the decomposition the surface of the coating layer with flaky corrosion product layer after corrosion.

4. CONCLUSION

This paper examined the morphology, corrosion performance and adhesion of Cu coatings on HDPE and ABS substrates. The following are the main findings of this work:

1. The Cu layer is deposited on HDPE and ABS successfully without deformation of the polymer structure.
2. Air cooling and bond coating are used to produce a more homogeneous coating structure and prevent the degradation of polymer.
3. The surface of the uncoated ABS sample was hydrophilic and had superior wettability and adhesiveness to the uncoated HDPE sample, which had a contact angle of 57.227°.
4. The adhesion strength between the ABS substrate and the Cu coating was greater than that between the HDPE substrate and the Cu coating.
5. A Tafel diagram for the Cu coating on the HDPE and ABS polymeric substrates revealed that the coating layer on the ABS substrate was denser and less porous than that on the HDPE substrate.
6. SEM images obtained after the corrosion of the Cu coating indicated that the surface of the coating after corrosion decomposed, resulting in a high surface roughness.
7. XRD data obtained after the corrosion test revealed that corrosion products covered the Cu surface.

8. The Cu layer on the ABS substrate had higher electrical conductivity than that of the Cu layer on the HDPE substrate.

9. In future research, it is possible to strengthen the polymer used as a substrate with fibers or particles before the coating process for comparison with the current research.

ACKNOWLEDGMENTS

The authors thank the Chemical Engineering Department / University of Technology for conducting Contact Angle Test and ACT Company in Basra / Iraq for performing pull off test on the samples used in this study.

REFERENCES

[1] Faupel, F., Zaporojtchenko, V., Strunskus, T., Erichsen, J., Dolgner, K., Thran, A., Kiene, M. (2002). Fundamental aspects of polymer metallization. Metallization of Polymers 2, 73-96. https://doi.org/10.1007/978-1-4615-0563-1_8

[2] Ganesan, A., Yamada, M., Fukumoto, M. (2014). The effect of CFRP surface treatment on the splat morphology and coating adhesion strength. Journal of Thermal Spray Technology, 23: 236-244. https://doi.org/10.1007/s11666-013-0003-z

[3] Melentiev, R., Yudhanto, A., Tao, R., Vuchkov, T., Lubineau, G. (2022). Metallization of polymers and composites: State-of-the-art approaches. Materials & Design, 221: 110958. https://doi.org/10.1016/j.matdes.2022.110958

[4] Gonzalez, R., Ashrafizadeh, H., Lopera, A., Mertiny, P., Mcdonald, A. (2016). A review of thermal spray metallization of polymer-based structures. Journal of Thermal Spray Technology, 25: 897-919. https://doi.org/10.1007/s11666-016-0415-7

[5] Faupel, F., Strunskus, T., Kiene, M., Thran, A., Bechtolsheim, C.V., Zaporojtchenko, V. (1998). Fundamental aspects of polymer metallization. MRS Online Proceedings Library, 511: 15-26. https://doi.org/10.1557/PROC-511-15

[6] Nguyen, L.H., Straub, M., Gu, M. (2005). Acrylate‐based photopolymer for two‐photon microfabrication and photonic applications. Advanced Functional Materials, 15(2): 209-216. https://doi.org/10.1002/adfm.200400212

[7] Chiu, P.G., Hsu, D.T., Kim, H.K., Shi, F.G., Nalwa, H.S., Zhao, B. (2001). Low-k materials for microelectronics interconnects. In Handbook of Advanced Electronic and Photonic Materials and Devices, pp. 201-234. https://doi.org/10.1016/B978-012513745-4/50041-X

[8] Matrood, G.J., Al-Gaban, A.M., Yousif, H.M. (2020). Studying the erosion corrosion behavior of NiCrAlY coating layer applied on AISI 446 stainless steel using thermal spray technique. Engineering and Technology Journal, 38(11A): 1676-1683. https://doi.org/10.30684/etj.v38i11A.1691

[9] Nouri, A., Sola, A. (2019). Powder morphology in thermal spraying. Journal of Advanced Manufacturing and Processing, 1(3): e10020. https://doi.org/10.1002/amp2.10020

[10] Fauchais, P., Montavon, G., Bertrand, G. (2010). From powders to thermally sprayed coatings. Journal of Thermal Spray Technology, 19: 56-80. https://doi.org/10.1007/s11666-009-9435-x

[11] Balić, E.E., Hadad, M., Bandyopadhyay, P.P., Michler, J. (2009). Fundamentals of adhesion of thermal spray coatings: Adhesion of single splats. Acta Materialia, 57(19), 5921-5926. https://doi.org/10.1016/j.actamat.2009.08.042

[12] Butt, M.A., Chughtai, A., Ahmad, J., Ahmad, R., Majeed, U., Khan, I. (2008). Theory of adhesion and its practical implications. Journal of Faculty of Engineering & Technology, 2007-2008: 21-45.

[13] Verma, R., Suri, N.M., Kant, S. (2017). Effect of parameters on adhesion strength for slurry spray coating technique. Materials and Manufacturing Processes, 32(4): 416-424. https://doi.org/10.1080/10426914.2016.1221090

[14] Revie, R.W. (2008). Corrosion and Corrosion Control: An Introduction to Corrosion Science and Engineering. John Wiley & Sons.

[15] Bobic, B., Mitrovic, S., Babic, M., Bobic, I. (2010). Corrosion of metal-matrix composites with aluminium alloy substrate. Tribology in Industry, 32(1): 3-11.

[16] Hillman, C., Castillo, B., Pecht, M. (2003). Diffusion and absorption of corrosive gases in electronic encapsulants. Microelectronics Reliability, 43(4): 635-643. https://doi.org/10.1016/S0026-2714(02)00315-3

[17] Zhao, P., Pecht, M. (2003). Field failure due to creep corrosion on components with palladium pre-plated leadframes. Microelectronics Reliability, 43(5): 775-783. https://doi.org/10.1016/S0026-2714(03)00064-7

[18] Wagner, S., Hoeppner, K., Toepper, M., Wittler, O., Lang, K.D. (2014). A critical review of corrosion phenomena in microelectronic systems. In PCIM Europe 2014; International Exhibition and Conference for Power Electronics, Intelligent Motion, Renewable Energy and Energy Management, Nuremberg, Germany, pp. 1-7. https://ieeexplore.ieee.org/document/6841343

[19] Vimala, J., Natesan, M., Rajendran, S. (2009). Corrosion and protection of electronic components in different environmental conditions-An overview. The Open Corrosion Journal, 2(1): 105-113. http://doi.org/10.2174/1876503300902010105

[20] Klengel, S., Stpehan, T., Spohn, U. (2017). A new method for prediction of corrosion processes in metallization systems for substrates and electrical contacts. In 2017 IEEE 67th Electronic Components and Technology Conference (ECTC), Orlando, FL, USA, pp. 1165-1170. https://doi.org/10.1109/ECTC.2017.139

[21] Tait, W.S. (2018). Electrochemical corrosion basics. In Handbook of Environmental Degradation of Materials, pp. 97-115. https://doi.org/10.1016/B978-0-323-52472-8.00005-8

[22] de la Fuente, D., Simancas, J., Morcillo, M. (2008). Morphological study of 16-year patinas formed on copper in a wide range of atmospheric exposures. Corrosion Science, 50(1): 268-285. https://doi.org/10.1016/j.corsci.2007.05.030

[23] Zhang, Q., Zhu, Z., Liu, P., Zhang, J., Cao, F. (2019). Corrosion electrochemical kinetic study of copper in acidic solution using scanning electrochemical microscopy. Journal of The Electrochemical Society, 166(13): C401. https://doi.org/10.1149/2.0061913jes

[24] Hoshi, Y., Oda, T., Shitanda, I., Itagaki, M. (2017). Communication—Real-time surface observation of

copper during anodic polarization with channel flow double electrode. Journal of The Electrochemical Society, 164(7): C450. https://doi.org/10.1149/2.0071709jes

[25] Langley, A.R., Carta, M., Malpass-Evans, R., McKeown, N.B., Dawes, J.H., Murphy, E., Marken, F. (2018). Linking the Cu (II/I) potential to the onset of dynamic phenomena at corroding copper microelectrodes immersed in aqueous 0.5 M NaCl. Electrochimica Acta, 260: 348-357. https://doi.org/10.1016/j.electacta.2017.12.083

[26] Björkbacka, Å., Johnson, C.M., Leygraf, C., Jonsson, M. (2017). Radiation induced corrosion of copper in humid air and argon atmospheres. Journal of The Electrochemical Society, 164(4): C201. https://doi.org/10.1149/2.1331704jes

[27] Roberge, P.R., Klassen, R.D., Haberecht, P.W. (2002). Atmospheric corrosivity modeling—A review. Materials & Design, 23(3): 321-330. https://doi.org/10.1016/S0261-3069(01)00051-6

[28] Whitesides, G.M. (2005). Nanoscience, nanotechnology, and chemistry. Small, 1(2): 172-179. https://doi.org/10.1002/smll.200400130

[29] Akkar, H.A., Khalooq, S. (2014). Characteristics and evaluation of nano electronic devices. Engineering and Technology Journal, 32(3): 486-497.

[30] Baer, D.R., Amonette, J.E., Engelhard, M.H., Gaspar, D.J., et al. (2008). Characterization challenges for nanomaterials. Surface and Interface Analysis, 40(3-4): 529-537. https://doi.org/10.1002/sia.2726

[31] Owen, S.R., Harper, J.F. (1999). Mechanical, microscopical and fire retardant studies of ABS polymers. Polymer Degradation and Stability, 64(3): 449-455. https://doi.org/10.1016/S0141-3910(98)00150-5

[32] Jalal, S.R. (2015). Comparison of shear properties for high density polyethylene (HDPE) and poly vinyl cloride (PVC) Polymers. Engineering and Technology Journal, 33(9A): 2039-2048.

[33] Devaraj, S., McDonald, A., Chandra, S. (2021). Metallization of porous polyethylene using a wire-arc spray process for heat transfer applications. Journal of Thermal Spray Technology, 30: 145-156. https://doi.org/10.1007/s11666-020-01119-1

[34] Voyer, J., Schulz, P., Schreiber, M. (2008). Electrically conductive flame sprayed aluminum coatings on textile substrates. Journal of Thermal Spray Technology, 17(5): 818-823. https://doi.org/10.1007/s11666-008-9228-7

[35] Ashrafizadeh, H., Mertiny, P., McDonald, A. (2015). Evaluation of the influence of flame spraying parameters on microstructure and electrical conductivity of Al-12Si coatings deposited on polyurethane substrates. In ITSC2015, pp. 370-376. https://doi.org/10.31399/asm.cp.itsc2015p0370

[36] Huang, W., Zhao, Y., Fan, X., Meng, X., et al. (2013). Effect of bond coats on thermal shock resistance of thermal barrier coatings deposited onto polymer matrix composites via air plasma spray process. Journal of Thermal Spray Technology, 22: 918-925. https://doi.org/10.1007/s11666-013-9942-7

[37] Matrood, G.J., Abdulkader, N.J., Ali, N.M. (2024). Determination of electrical conductivity of aluminum nano films prepared by flame thermal spray. Iraqi Journal of Applied Physics, 20(2B): 453-456. https://www.iasj.net/iasj/download/e4cd39797132e1ec.

[38] Mohsin, A.N., Yousif, H.M., Ahmed, S.S. (2021). Investigation of the diffusion depth of Ni-Cu thermal spray coating for the low carbon steel. Engineering and Technology Journal, 39(11): 1734-1739. https://doi.org/10.30684/etj.v39i11.2179

[39] Edan, F.H. (2016). Prediction of contact angle for sintered alloy for solid freeform fabrication. Engineering & Technology Journal, 34(8): 1666-1672. https://doi.org/10.30684/etj.34.8A.16

[40] Bogdanova, Y.G., Dolzhikova, V.D., Alentiev, A.Y., Karzov, I.M. (2012). Contact angle measurements in study of polymers for creation of materials. Journal of International Scientific Publications: Materials, Methods & Technologies, 6: 273-285.

[41] Ramos, N.M.M., Simões, M.L., Delgado, J.M.P.Q., De Freitas, V.P. (2012). Reliability of the pull-off test for in situ evaluation of adhesion strength. Construction and Building Materials, 31: 86-93. https://doi.org/10.1016/j.conbuildmat.2011.12.097

[42] Bai, Y., Basheer, P.A.M., Cleland, D.J., Long, A.E. (2009). State-of-the-art applications of the pull-off test in civil engineering. International Journal of Structural Engineering, 1(1): 93-103. https://doi.org/10.1504/IJStructE.2009.030028

[43] Mohammad, L.N., Bae, A., Elseifi, M.A., Button, J., Scherocman, J.A. (2009). Evaluation of bond strength of tack coat materials in field: Development of pull-off test device and methodology. Transportation Research Record, 2126(1): 1-11. https://doi.org/10.3141/2126-01

[44] Croll, S.G., Siripirom, C., Keil, B.D. (2014). Pull-off adhesion test for coatings on large pipes: possible variations in failure location and mode. In Pipelines 2014: From Underground to the Forefront of Innovation and Sustainability, pp. 1319-1333. https://doi.org/10.1061/9780784413692.119

[45] Dong, L., Yang, F., Yu, T., Zhang, N., Zhou, X., Xie, Z., Fang, F. (2023). Contribution of grain boundary to strength and electrical conductivity of annealed copper wires. Journal of Materials Research and Technology, 26: 1459-1468. https://doi.org/10.1016/j.jmrt.2023.08.012

[46] Tazegul, O., Dylmishi, V., Cimenoglu, H. (2016). Copper matrix composite coatings produced by cold spraying process for electrical applications. Archives of Civil and Mechanical Engineering, 16(3): 344-350. https://doi.org/10.1016/j.acme.2016.01.005

[47] Alfantazi, A.M., Ahmed, T.M., Tromans, D. (2009). Corrosion behavior of copper alloys in chloride media. Materials & Design, 30(7): 2425-2430. https://doi.org/10.1016/j.matdes.2008.10.015

[48] Liao, X., Cao, F., Zheng, L., Liu, W., Chen, A., Zhang, J., Cao, C. (2011). Corrosion behaviour of copper under chloride-containing thin electrolyte layer. Corrosion Science, 53(10): 3289-3298. https://doi.org/10.1016/j.corsci.2011.06.004